Studies of Monomode Long Wavelength Fiber Systems at the British Telecom Research Laboratories

JOHN E. MIDWINTER, MEMBER, IEEE

Abstract—**The key components of long wavelength monomode systems to operate in the 1300 and 1550 nm windows have been under study for some years to establish the best combination of operating parameters for intercity land and undersea use. Recently, two prototype systems have been assembled with 37 and 49 km repeater spacings, operating at 140 Mbits/s and at 1300 and 1500 nm, respectively. Higher bit rate systems are also under study.**

Introduction

THE possibility of very low attenuation fibers in the 1300 and 1550 nm wavelength windows raises the possibility of fiber transmission systems operating with exceptionally long repeater spacings in the 30–100 km range. Such systems would lend themselves to application either on intercity long-haul or undersea routes. In both cases, high bit rate operation seems desirable, at 140 Mbits/s or above, so that very stringent requirements arise for the fiber bandwidth. Consequently, we have linked long wavelength operation with monomode fiber for some time. This paper attempts to review the major activities under this program and to highlight its achievements. The work falls naturally into a number of largely separate activities which come together in the demonstration of monomode high bit rate transmission over a complete assemblage of the subcomponents. We will first review the component activities.

The Transmission Medium

The attenuation characteristics of the recent BTRL fiber have been described in detail in an accompanying paper [1]. A major theme of our work has been the optimum design of a monomode fiber for use in either the 1300 or 1550 nm windows. It is clear that this is a complex process, involving not only the optimization of the attenuation but also the dispersion for a particular application, the spot size for jointing or launching, and the sensitivity to microbending loss on cabling. It is also desirable to establish a fiber design that is relatively insensitive to fluctuations in manufacturing parameters that are difficult to control if high production yield is to ensue.

The major results obtained on the fabrication of monomode fibers can be summarized as follows. It is now possible to achieve on a routine basis attenuation of 0.4 dB/km at 1300 nm in a fiber having zero first-order dispersion close to this wavelength. It has also been possible to achieve an attenuation of 0.37 dB/km at 1550 nm in a fiber having the zero first-order dispersion shifted to about 1500 nm. Lower attenuations are possible at this wavelength with a smaller degree of shift of the zero of dispersion. The water peak in the fiber at 1400 nm has been reduced to a height above the baseline of 2–4 dB/km by very careful materials processing. Fibers of this type can be fabricated in continuous lengths of 15–20 km. The detailed fabrication of these fibers is discussed in the associated paper [1] and will not be discussed further here. Careful measurements have been made of all the key parameters controlling their performance and these data have been used to model their performance and to check the existing theories for monomode propagation.

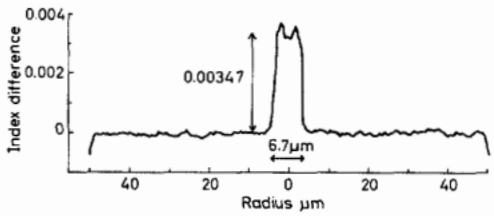


Fig. 1. Measured profile for a monomode fiber using the refracted near-field technique.

One important feature of the fiber from a propagation point of view is the index profile. This is obtained, from the fiber itself, by the refracted ray technique [2]. Such a profile is shown in Fig. 1. This gives valuable information to the fiber maker in establishing the required deposition conditions. By obtaining two orthogonal profiles across the entire fiber diameter, separations of the core and cladding centers as small as 0.1 μm can be measured which allows the prediction of splice losses.

Pulses with a $1/e$ width of 230 ps produced by an Nd:YAG laser operating at 1.32 μm have been used to determine the monochromatic impulse response of our fibers. The spectral width of this source is sufficiently small for material and waveguide dispersion to be neglected. Fibers of various lengths have been studied. In a typical study, the input and output pulsewidths both lay in the range of 230 ±10 ps for two fibers spliced to a total length of 27 km. Thus, the monochromatic pulse spreading, arising from birefringence or other mode dispersive effects, was certainly less than 4 ps/km, not a significant problem for current telecommunications applications.

The availability of low attenuation monomode fiber has enabled us to establish an efficient fiber Raman source for the

Manuscript received December 5, 1980; revised January 12, 1981.
The author is with the British Telecom Research Laboratories, Ipswitch, Suffolk IP5 7RE, England.

0018-9197/81/0600-0911$00.75 © 1981 IEEE

Authorized licensed use limited to: British Telecommunications via the BT Library. Downloaded on July 21,2025 at 17:03:29 UTC from IEEE Xplore. Restrictions apply.

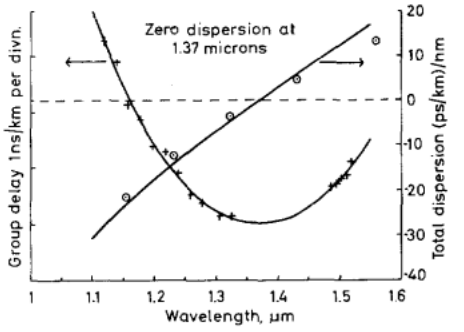


Fig. 2. Calculated (circles) and measured (crosses) showing group delay and dispersion data. The solid dispersion curve is obtained from the experimental group delay data.

1.06–1.7 μm range. Using it, spectral group delay measurements are obtained to which a linearized Sellmeier equation is fitted. The dispersion is obtained by differentiation as shown in Fig. 2. From the measured profile (Fig. 1), theoretical values of dispersion are calculated and presented as circles in Fig. 2. For this particular fiber at 1.30 μm, the $1/e^2$ field width is approximately 10 μm—almost half as much again as the core diameter. It is the field width rather than core diameter that is significant for fiber splicing. The same theory also predicts the cutoff of the LP_{11} mode as 870 nm, while the maximum of the mode cutoff peak on the total attenuation plot is seen at the same wavelength. However, the measured value will depend upon other factors, such as fiber bending radius and is not, therefore, absolute.

Fibers having significant shifts of minimum dispersion to longer wavelengths have also been made and their dispersion measured and modeled with equally good agreement. This is discussed in more detail in a companion paper [1]. The additional attenuation associated with the relatively high germania doping levels in these fibers has been identified as absorption rather than scattering by using a calorimetric absorption loss apparatus [3]. This has the sensitivity to measure 0.05 dB/km for 1 W of guided power. The difference between the total and absorption losses gives the scatter loss. It is worth noting that the conventional technique of plotting attenuation on a wavelength^{-4} scale does not necessarily separate the Rayleigh scatter component from the other attenuation mechanisms since the absorption arising from the germania color center [1] shows a wavelength dependence that is indistinguishable from wavelength^{-4} over small wavelength ranges.

An important parameter in fiber design is the microbending loss arising during packaging of the fiber and its dependence upon NA. Many approaches to packaging are possible, ranging from a tightly fitting extrusion [4] to a loose tube approach [5]. The latter can only cause extra attenuation when the structure is strained and curved so that the fiber is tensioned against the wall. We have investigated the effect of this strain on three monomode fibers of varying core diameters and index differences. A well established loose tube coating was used [5], with an initial pay-off reel back tension of 60 gm or around 0.1 percent strain. By rewinding the fiber from the 65 mm radius take-up drum to one of 500 mm, the fiber strain against the tube wall could be increased to about 0.25 percent strain.

The results are shown in Table I. It is apparent that two of the fibers show no measurable loss increment at 1300 or 1550 nm after the packaging process. The third fiber shows little added loss at 1300 nm but considerable loss at 1550 nm. This loss is further increased as the fiber strain is increased by the rewinding process. The three spectral losses for the primary coated, tubed, and rewound states are shown in Fig. 3 for this third fiber.

The fiber core diameters were measured from refracted ray profiles [2] and the NA's calculated as in [4]. In general, agreement with the findings of [4] (a tight extrusion process) is good, giving confidence that around 0.2 percent relative index difference and a V-value of about two represents a fiber design limit from the point of view of cabling loss.

Splicing Techniques and Connectors for Monomode Fibers

The development of a practical and reliable splicing technique which can be used in the field without the need for remote power monitoring is a key issue for monomode systems. Work has concentrated on the fusion arc technique which has been used with great success for multimode fibers.

Theoretical studies of the spot diameter as a function of the fiber design parameters have been made and compared with a wide range of experimentally measured fibers. Good agreement has been found so that there is confidence in using such data to model fiber joint losses. Independent experimental studies have been made of the joint losses using a limited range of fiber designs to test the theory.

Our experience, in common with that of other workers [6], has shown that the surface tension of the melted silica glass provides a high degree of self-alignment during the splicing process. Average splice losses of 0.3 dB are currently achieved for monomode fibers with 7 μm core diameters (100 μm cladding) operating at 1300 nm. The fusion splicing technique depends fundamentally for its success on the centrality of the fiber core within the cladding and these results were obtained using fibers with low concentricity errors. Significantly higher losses are obtained for fibers with poorer geometrical control. Present indications are that a tolerance of around 0.5 μm or less is likely to be required in order to yield splices with sufficiently low losses for practical systems. This will be an important target to be achieved in the fiber production environment.

Low loss splices are likely to be most important for inland trunk systems where the maximum cable installation length will be dictated by operational and logistical considerations. A spacing of around 1 km between splices will be desirable, although longer installation lengths could prove to be practicable. For submarine systems, spacings of several kilometers should be possible and therefore a smaller number of splices will be required for the equivalent regenerator section.

Detailed assessment of individual fusion joints has been attempted and it is clear that the actual losses achieved between a given pair of fibers depend upon several factors, including the accuracy with which the fiber end is cut perpendicular to the fiber axis and the fiber core/cladding concentricity. However, microscopic examination of selected joints shows that major distortion of the guiding core can occur through the

Authorized licensed use limited to: British Telecommunications via the BT Library. Downloaded on July 21,2025 at 17:03:29 UTC from IEEE Xplore. Restrictions apply.

TABLE I

Fiber	O/D	Core Diameter	LP_{11} Cutoff	NA	Δ percent (Relative)	V-values at λ 1.3 μm	V-values at λ 1.55 μm	Loss Increment at λ 1.3 μm	Loss Increment at λ 1.55 μm
1	125 μ	9.1 μ	1.24 μ	0.105	0.26	2.31	1.94	0	0
2	100 μ	6.3 μ	1.15 μ	0.135	0.43	2.05	1.74	0	0
3	100 μ	8.5 μ	1.05 μ	0.095	0.21	1.95	1.64	0.1 dB/km	5 dB/km (at 0.1 percent strain)

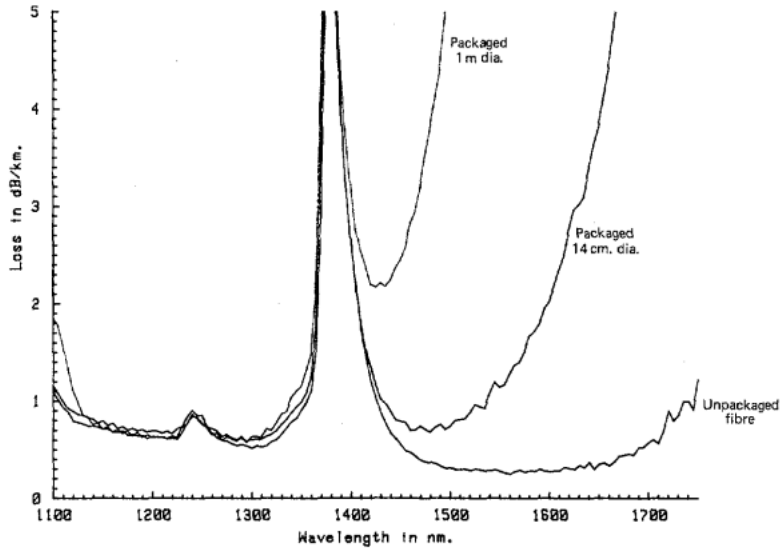


Fig. 3. Attenuation curves versus wavelength for the same fiber as drawn and after packaging when wound on different diameter drums.

joint region despite nominally good fiber precision and alignment. This effect is critically dependent upon the detailed design of the fusion jointing jig. Reproducible results are best achieved using a fully automated jointing jig in which both the arc and the fiber positioning are program controlled.

Work on monomode fiber connectors has centered on the use of bead lens termination of fibers and kinematic location techniques in order to circumvent the need for ultrahigh precision engineering. The formation of a bead lens [7] on the end of a previously cleaved fiber is performed by placing the fiber in the proximity of an electric arc discharge. Surface tension forces then cause the fiber material to flow producing a perfect, spherical flame polished lens.

The bead termination offers several advantages.

1) The bead acts as an alignment component within the ball cluster, significantly reducing the effects of fiber outside diameter tolerances.

2) Field expansion at the bead face produces a reduction in lateral offset tolerances for small loss penalty (Fig. 4).

3) Connectors employing bead termination lend themselves to field assembly without recourse to polishing.

4) Reflections from a bead termination are significantly below that from a plane ended fiber.

The triple ball connector has been initially used with the fiber bead termination technique [8]. A prototype connector (Fig. 5) has been developed which gives a stable loss of about 2 dB with a standard deviation of approximately 0.2 dB. Although

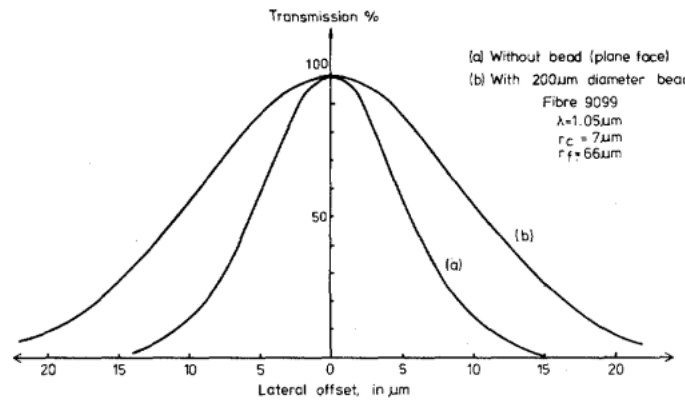


Fig. 4. Comparison of lateral offset tolerances for bead and plane ended monomode fibers.

relatively high loss, the connector has advantages of field assembly and potential low cost. The intrinsic loss, which is around 1.5 dB, occurs because the mechanical separation of the bead lenses, when nestled within the ball clusters, does not coincide with the optimum optical separation for practical monomode fibers.

Other connectors employing kinematic location techniques and bead lens termination are being investigated with a view to obtaining lower losses while retaining the assembly and low cost advantages.

Authorized licensed use limited to: British Telecommunications via the BT Library. Downloaded on July 21,2025 at 17:03:29 UTC from IEEE Xplore. Restrictions apply.

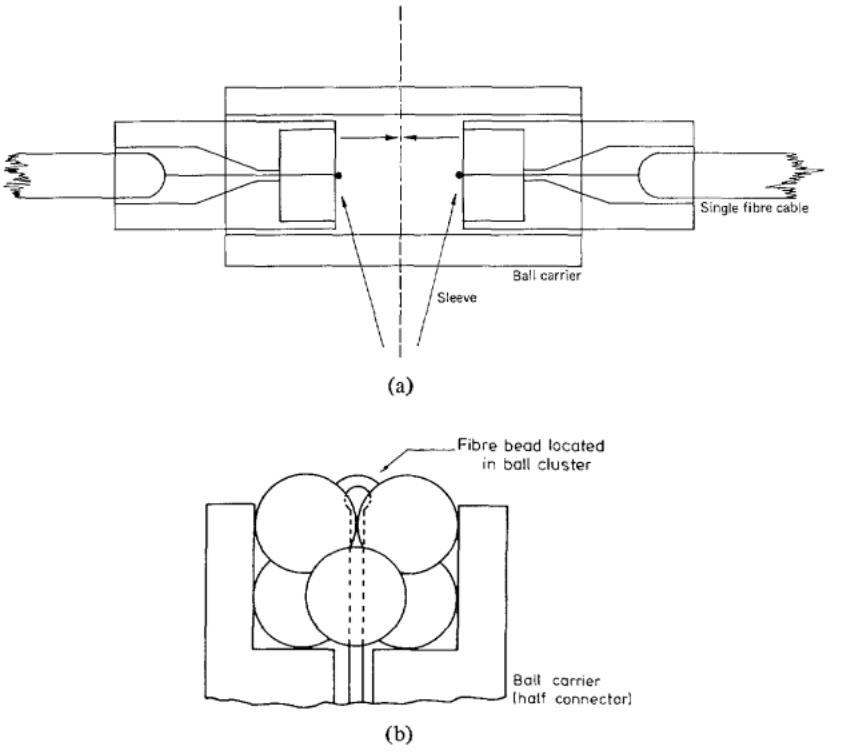


Fig. 5. (a) Schematic layout of the monomode bead-ended fiber connector. (b) Design of the ball alignment cluster showing bead location.

Sources and Transmitter Modules

The initial emphasis of the long wavelength laser development of BTRL has been on the optimization of oxide isolated stripe InGaAsP lasers for use in single-mode fiber systems operating at 1.3 μm. In view of the high temperature sensitivity of long wavelength lasers, particular attention has been paid to minimizing the thermal and electrical resistance, in the latter case by the use of Schottky contacts [9].

For practical applications of optical fiber systems, lasers as discrete components present serious problems of optical and electrical interfacing. We have previously reported [10] on a hybrid transmitter module for graded index fiber systems which greatly simplifies the use of lasers in high bit rate systems. The dual-in-line module (Fig. 6) incorporates a laser, a microlens for coupling the laser to the fiber tail, a hybrid laser modulation circuit, and a hybrid laser level control circuit. The control circuit [11], which employs a novel low frequency optical power monitoring technique, has been produced on a single bipolar integrated circuit. The operation of the control circuit is essentially independent of the modulation rate, and modules containing such a circuit have been operated successfully at modulation rates of up to 640 Mbits/s.

The control circuit operates from ±5 V, and the power consumption of a transmitter module containing a control circuit, a modulation circuit and a laser with a 75 mA threshold current, is approximately 600 mW.

Similar modules have been produced for single-mode fiber systems. The single-mode fiber tail is butt coupled to the laser, the fiber tail being positioned for maximum coupled power prior to being fixed to the laser submount using a metallic solder. The coupling efficiency to oxide isolated stripe lasers with stripe widths in the range of 10–20 μm is 10–15 percent.

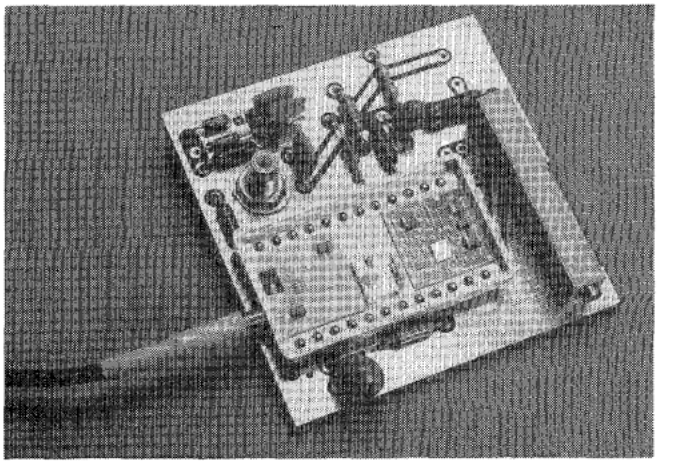


Fig. 6. Photograph showing the monomode hybrid transmitter module with integral control and drive circuits, monitor detector and laser to fiber interface.

Detector and Receiver Modules

The optical receivers, designed and developed at BTRL, for systems operating in the 1.2–1.6 μm wavelength region have been based on a very low capacitance InGaAs p-i-n photodiode hybrid integrated with a high input impedance GaAs MESFET preamplifier [12]–[14]. These p-i-n-FET hybrid receivers have demonstrated receiver sensitivities superior to either the germanium or III-V avalanche photodiodes reported to date [15]–[17]. In addition, these receivers have the significant operational advantages of being relatively temperature insensitive, and of requiring only low voltage supply rails.

The structure of the $In_{0.53}Ga_{0.47}As/InP$ p-i-n photodiode, suitable for operation up to a wavelength of 1.6 μm, is shown

Authorized licensed use limited to: British Telecommunications via the BT Library. Downloaded on July 21,2025 at 17:03:29 UTC from IEEE Xplore. Restrictions apply.

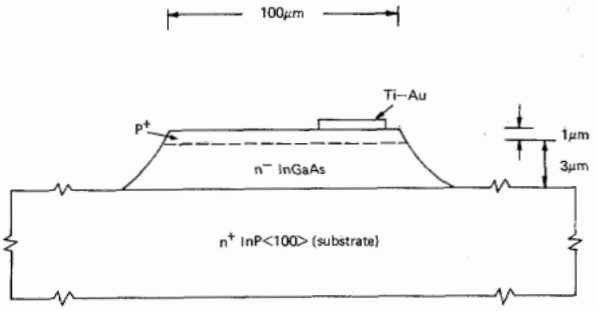


Fig. 7. Construction of the $In_{0.53}Ga_{0.47}As$ p-i-n photodiode grown on InP for operation out to a wavelength of 1600 nm.

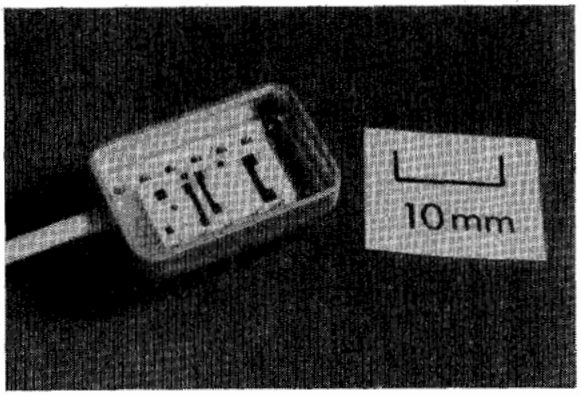


Fig. 8. A prototype hybrid receiver module using the p-i-n photodiode in conjunction with a GaAs FET preamplifier.

schematically in Fig. 7. The ternary layer is grown by the vapor-phase epitaxial chloride process and the indium/gallium ratio is chosen to ensure lattice matching to the n^+ InP substrate. The p-n junction is formed by zinc diffusion and the active area of the photodiode, having a diameter of 100 μm, is defined by mesa etching. The doping concentration of the ternary layer is reproducibly $1\text{-}3.10^{15}$ cm^{-3} giving a diode capacitance at -10 V bias of 0.3 pF. The external quantum efficiency without antireflection coating, over the wavelength range of 1.2–1.6 μm, is 40–50 percent for top-entry illumination and 70–80 percent for rear-entry illumination through the InP substrate. The room temperature leakage current is typically less than 10 nA at -10 V bias.

The receiver module design is shown in Fig. 8. The p-i-n photodiode and GaAs MESFET preamplifier are hybrid integrated on a $\frac{1}{4} \times \frac{1}{2}$ in thick film circuit which is soldered into a standard DIL metal package. The preamplifier circuit is a high input impedance FET-bipolar cascode with an emitter follower buffer and differentiating capacitor. The GaAs MESFET is a Plessey GAT 5 giving a total input capacitance for the receiver due to the p-i-n, FET gate-source, and stray capacitances of 0.7 pF. The photodiode load resistor is 2 MΩ and, consequently, the long input *RC* time constant is compensated by the differentiating capacitor prior to the second stage gain. The voltage supply rails required for the module are +10 V and -5 V.

The receiver sensitivity at 1.3 μm wavelength is shown in Fig. 9, for a module incorporating an InGaAs p-i-n having a quantum efficiency of 40 percent. The receiver sensitivities, corresponding to an error rate of 10^{-9}, were determined experimentally between 34 and 320 Mbits/s and show close

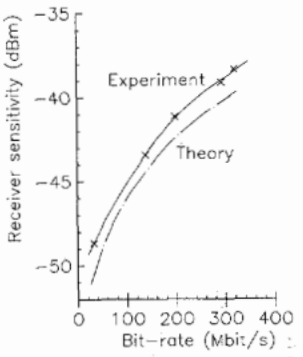


Fig. 9. Receiver sensitivity of the hybrid p-i-n–FET module at 1300 nm as a function of bit rate for 10^{-9} error rate.

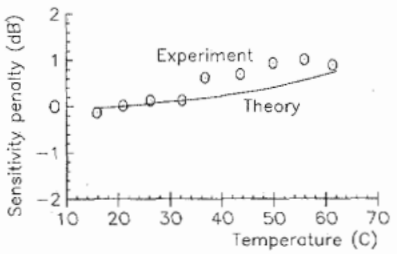


Fig. 10. Variation of sensitivity with temperature of the hybrid p-i-n FET receiver when operating at 140 Mbits/s, 1300 nm, and 10^{-9} error rate.

agreement with the theoretically predicted performance. The temperature dependence of the receiver sensitivity for a 140 Mbits/s system is shown in Fig. 10 and indicates a performance degradation of only 1 dB between 10 and 60°C.

System Studies

Using a selection of the components and subassemblies described above, two experimental systems have been assembled and studied. Both were operated initially at 140 Mbits/s, although the receiver regenerator was capable of operation at any bit rate in the range of 30–300 Mbits/s. One experiment was conducted at 1300 nm over a continuous length of 37 km of monomode fiber while the other was operated at 1500 nm over 49 km of monomode fiber. A common receiver regenerator was used for both studies as shown in Fig. 11.

An NRZ $2^{10} - 1$ pseudorandom binary signal at 140 Mbits/s was applied to the laser driver which comprised a GaAs MESFET connected in shunt configuration with the laser. The IC level controller [11] automatically adjusts the bias and drive currents fed to the laser such that the laser output is essentially stabilized against temperature and aging effects.

The monomode fiber was connected to the multimode fiber pigtail of the receiver by a rod lens connector. This comprised two identical thick plano-convex lenses with the fiber ends placed at their axial foci. When brought together on a common axis the output from the monomode fiber was imaged within the core of the multimode fiber.

The low level, uniform amplitude signal obtained from the p-i-n–FET receiver after the differentiating capacitor [14] was fed to a 30 dB wide-band amplifier. The signal level was then sufficient, after low pass filtering, to drive a high speed comparator (Plessey SP9685) to ECL logic levels at its output. This comparator, with its large signal handling capability, allows

Authorized licensed use limited to: British Telecommunications via the BT Library. Downloaded on July 21,2025 at 17:03:29 UTC from IEEE Xplore. Restrictions apply.

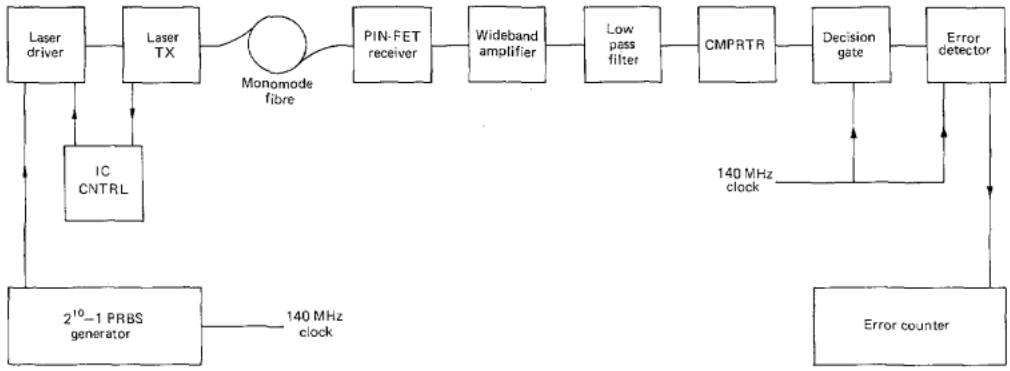


Fig. 11. Layout of prototype monomode 1300/1500 nm system.

TABLE II
SYSTEM RESULTS SUMMARY

	1.3 μm	1.5 μm
Link length	37 km	49 km
Path loss	~29 dB	~24 dB
Laser wavelength	1.275 μm	1.51 μm
Coupled laser power	~−11 dBm	~−15 dBm
Extinction ratio penalty	0.2 dB	1.8 dB
Received power	−40 dBm	−39 dBm
System margin	~3 dB	~3 dB

wide dynamic range to be achieved without introducing age. The three pole Butterworth low pass filter was designed to closely approximate the transfer function required to produce a full raised-cosine frequency-domain response when an NRZ rectangular optical pulse is incident at the receiver. The clocked *D* type bistable decision gate retimed and regenerated the output pulses from the comparator. The output from the decision gate was then fed to an error detector and counter.

A summary of system performance at 1.3 μm using a laser transmitter module with monomode fiber pigtail is given in Table II.

An experiment was also performed at 1.5 μm using an STL 20 μm stripe GaInAsP stud mounted laser [18]. The output from the laser was coupled into the monomode fiber using an imaging system. The link length was extended with a further 12 km of fiber to 49 km by a third fusion splice. System performance is summarized in Table II.

The error rate curves for the two experiments Figs. 12 and 13 were obtained by inserting optical attenuation at the receiver connector and recording the error rate and mean photocurrent. It can be seen from Fig. 12 that performance at 1.3 μm over 37 km is virtually identical to that over 1 m, demonstrating the very low level of dispersion at this wavelength.

During the course of this experiment, periods of high error rate were experienced resulting in no effective system margin. On further investigation it was found that the effect was related to dynamic instabilities in the optical pulses from the laser transmitter. Reflections back into the lasing cavity were thought to be responsible for this phenomenon.

From Fig. 13 it can be seen that a penalty of only 0.7 dB is paid for operation over 49 km at 1.51 μm, indicating that dispersion related effects arising from the 4 nm laser linewidth are still small in this wavelength region.

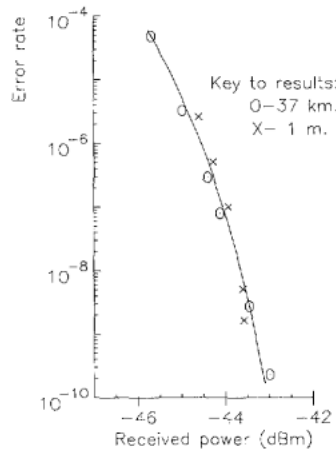


Fig. 12. Measured error rate curves for the system using an InGaAs p-i-n-FET receiver operating at 140 Mbits/s and 1300 nm with and without 37 km of monomode fiber.

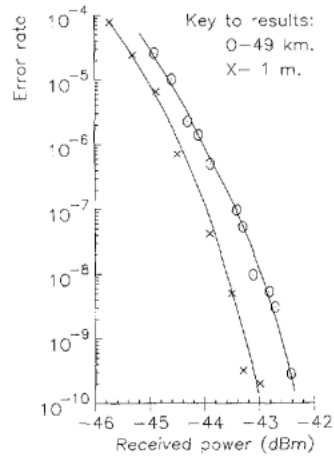


Fig. 13. Measured error rate curves for the system using an InGaAs p-i-n-FET receiver operating at 140 Mbits/s and 1500 nm with and without 49 km of monomode fiber.

System experiments over an undersea monomode fiber cable have also been performed in the United Kingdom after the successful laying of a 10 km trial section in Loch Fyne on the west coast of Scotland in February 1980 [19]. This work was carried out under a joint BTRL/STC development program. The cable, which was made by STC, contained four multimode and two monomode fibers. Transmission tests over one of the

Authorized licensed use limited to: British Telecommunications via the BT Library. Downloaded on July 21,2025 at 17:03:29 UTC from IEEE Xplore. Restrictions apply.

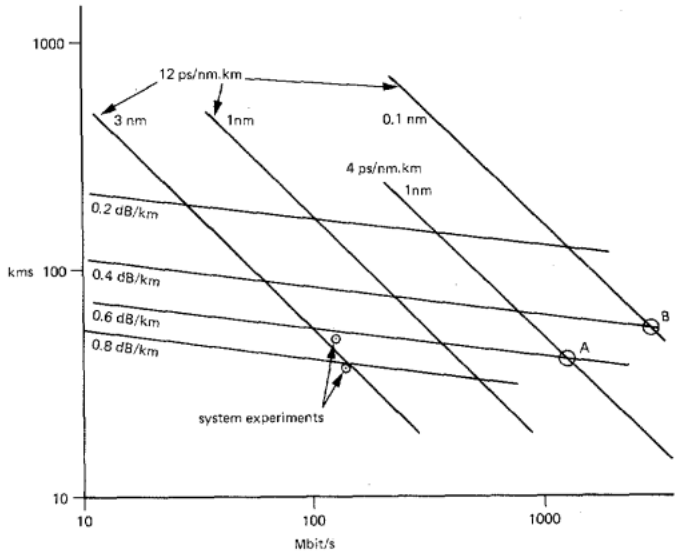


Fig. 14. Theoretical plot of repeater spacings versus bit rate and some limitations arising from dispersion and attenuation as discussed in the text.

monomode fibers were made at 160, 280, and 320 Mbits at a wavelength of 1.3 μm. At each of the transmission speeds an error rate of less than 1 in 10^9 was achieved over the 10 km loop.

Summary

Our studies have shown that the design of an optimum fiber for systems use is complex. Not only do the attenuation and dispersion characteristics have to be born in mind, but also the dependence of the cable microbending loss, the joint loss, and the launching efficiency. In assessing these factors, it is also necessary to consider the ease and reproducibility of the fabrication process since high yield will be required.

The coupling of the laser to a monomode fiber can be achieved within the framework of a simple transmitter module design but optical power instabilities can easily arise if reflections occur. Several approaches are currently under study to overcome these problems. The use of the hybrid p-i-n-FET receiver yields both excellent performance with great versatility and simplicity of circuit design, avoiding the need for the high voltage supplies associated with avalanche detectors. The temperature stability of these receivers is also excellent.

Studies of the complete systems in the laboratory have shown that the combination of exceptionally low attenuation with very low dispersion allows high bit operation over very long repeater sections, with 49 km at 140 Mbits/s being demonstrated. However, these exciting results should not draw attention away from the fact that to achieve them in a fully engineered form still requires considerable further development and very close control of all the manufacturing tolerances, both in the fiber, the cable, and the repeater optoelectronic and electronic devices.

In Fig. 14, we have attempted to pull together some of the themes presented in this paper. We have seen that fiber attenuation of 0.2–0.4 dB/km can be achieved, respectively, in the 1500 and 1300 nm wavebands, provided that the zero of dispersion is left unshifted from the 1300 nm region. Allowing an additional 0.2 dB/km for joint and cable attenuation, we arrive at target attenuations of 0.4 and 0.6 dB/km for the transmission medium. The transmitter power is likely to range between 0 and +3 dBm, but allowing for a low launching efficiency, −10 dBm seems realistic if stable operation is to ensue. The receiver sensitivity is given approximately (see Fig. 9) by $-(65 - 10 \log_{10} M)$ dBm where M is in megabits per second, so that the power available to the system is given roughly by $(55 - 10 \log_{10} M)$ dB. The power limited repeater spacing curves in Fig. 13 have been derived using this relationship.

Mode partition noise [20] has been suggested as the major dispersion limiting factor in a monomode fiber system. In our own 49 km transmission study, the fiber dispersion was measured to be 12 ps/nm · km and the source linewidth in the region of 3–4 nm. A small receiver power penalty was observed and ascribed to this effect. On this basis, we have set an arbitrary dispersion limitation at the $\frac{1}{5}$ bit interval and the dispersion curves of Fig. 14 are drawn using this relation. The curve for 4 ps/nm · km dispersion is taken as a conservative figure for operation within the "zero" dispersion region, while the 12 ps/nm · km figure is our own figure for a fiber operated at 1500 nm but with the zero of dispersion near to 1300 nm. Several factors now emerge from these curves.

Very long repeater spacings, greater than 100 km, are clearly theoretically possible but would require exceptionally tight control of the fiber cable and joint attenuation. For land systems, such very long repeater spacings are probably not justified. Operation with an attenuation of 0.6 dB/km at 1300 nm probably results in simultaneous dispersion and bandwidth limitation at around 40 km and 1 Gbit/s (point *A* on the figure). Using the same fiber in the 1500 nm window but with a superior (0.1 nm linewidth) laser pushes this point to 55 km and 3 Gbits/s. It is thus our conclusion that for land system applications of monomode fibers, the likely development sequence is as follows. The first systems will operate in the 1300 nm waveband but with fiber cables designed to minimize the attenuation in the 1500 nm window also. Without any special attempts to shift the zero of dispersion, 30 km operation at a few 100 Mbits/s will be quite feasible. Provided a substantial power margin has been left, the same cable will be capable of upgrading to higher bit rate operation by as much as a factor of 10 as the laser and electronics technology advances. From an engineering point of view, this appears to be a much more attractive route than trying to push for ever longer repeater spacings, and in the United Kingdom at least, achievement of 30 km spacing would result in the housing of all electronic equipment within existing buildings. In the case of undersea applications, the conclusion reached will be much more route dependent. If routes exist of 100–150 km length, then a major motivation will exist for the achievement of a repeaterless system. However, for very long haul routes (1000–2500 km), repeaters will again be required and the motivation to push for the ultimate spacing is likely to be subjugated to the desire to have a system that is readily manufacturable with substantial engineering margins, leading again to a system close to the land system suggested above.

Authorized licensed use limited to: British Telecommunications via the BT Library. Downloaded on July 21,2025 at 17:03:29 UTC from IEEE Xplore. Restrictions apply.

In the very long term, further expansion of the traffic carrying capability of a monomode fiber system is conceivable through the use of monomode integrated optic devices providing wavelength multiplexing facilities. Monomode fiber systems operating in the longer wavelength windows of the silica fiber system thus offer great potential for long haul telecommunications of the future. The time scales for their commercial realization are open to debate but early field experiments seem certain and the laboratory test bed systems have already demonstrated the possibilities.

Acknowledgment

The author wishes to acknowledge the assistance of his colleagues in preparing the paper and the Director of Research, British Telecom, for permission to publish it.

References

[1] B. J. Ainslie, K. J. Beales, C. R. Day, and J. D. Rush, "Interplay of design parameters and fabrication conditions on the performance of monomode fibers made by MCVD," this issue pp. 854–857.

[2] K. I. White, "Practical application of the refracted near-field technique for the measurement of optical fibre refractive index profiles," *Opt. Quantum Electron.*, vol. 11, pp. 185–196, Mar. 1979.

[3] —, "A calorimetric method for the measurement of low optical absorption losses in optical communication fibres," *Opt. Quantum Electron.*, vol. 8, pp. 73–75, Jan. 1975.

[4] Y. Katsuyama, S. Mochizuki, K. Ishihara, and Y. Ishida, "Single mode optical fibre cable," *Rev. ECL*, vol. 27, pp. 507–514, Aug. 1979.

[5] L. A. Jackson, M. H. Reeve, and A. G. Dunn, "Optical fiber packaging in loose fitting tubes of orientated polymer," *Opt. Quantum Electron.*, vol. 9, pp. 493–498, Nov. 1977.

[6] I. Hatakeyama and H. Tsuchiya, "Fusion splices for single mode optical fibers," *IEEE J. Quantum Electron.*, vol. QE-14, pp. 614–619, Aug. 1978.

[7] D. B. Payne and C. A. Millar, "Triple ball connector using fibre bead location," *Electron. Lett.*, vol. 16, pp. 11–12, Jan. 3, 1980.

[8] C. A. Millar and D. B. Payne, "Monomode fibre connector using fibre bead location," in *Proc. 6th European Conf. Opt. Commun.*, York, England, Sept. 1980.

[9] A. G. Steventon, R. E. Spillett, R. E. Hobbs, M. G. Burt, P. J. Fiddyment, and J. V. Collins, "CW operation of GaInAsP stripe lasers," *IEEE J. Quantum Electron.*, vol. QE-17, pp. 602–610, May 1981.

[10] K. H. Cameron, M. R. Matthews, K. R. Preston, and D. W. Smith, "A hybrid laser transmitter module for use in optical fibre systems," presented at the 30th Electron. Components Conf., San Francisco, CA, Apr. 1980.

[11] D. W. Smith and T. G. Hodgkinson, "Laser level control for high bit rate optical fibre systems," presented at the 13th Circuits Syst. Int. Symp., Houston, TX, Apr. 1980.

[12] D. R. Smith, R. C. Hooper, K. Ahmad, D. Jenkins, A. W. Mabbitt, and R. Nicklin, "PIN-FET hybrid optical receiver for longer wavelength optical communication systems," *Electron. Lett.*, vol. 16, pp. 69–71, Jan. 17, 1980.

[13] D. R. Smith, A. K. Chatterjee, M. A. Z. Rejman, D. Wake, and B. R. White, "PIN-FET hybrid optical receiver for 1.1 to 1.6 μm optical communication systems," *Electron. Lett.*, vol. 16, pp. 750–751, Sept. 11, 1980.

[14] R. C. Hooper, M. A. Z. Rejman, S. T. D. Ritchie, D. R. Smith, and B. R. White, "PIN-FET hybrid optical receivers for longer wavelength optical communication systems," presented at the 6th European Conf. Opt. Commun., York, England, Sept. 1980.

[15] M. C. Brain, "Responsivity and noise characterisation of Ge avalanche photodiode throughout wavelength range 1.1 to 1.7 μm," *Electron. Lett.*, vol. 15, pp. 821–823, Dec. 6, 1979.

[16] O. Mikami, H. Ando, H. Kanbe, T. Mikawa, T. Kaneda, and Y. Toyama, "Improved germanium avalanche photodiodes," *IEEE J. Quantum Electron.*, vol. QE-16, pp. 1002–1007, Sept. 1980.

[17] N. Susa, H. Nakagome, O. Mikami, H. Ando, and H. Kanbe, "New InGaAs/InP avalanche photodiode structure for 1.0 to 1.6 μm wavelength region," *IEEE J. Quantum Electron.*, vol. QE-16, pp. 864–870, Aug. 1980.

[18] G. D. Henshall and P. D. Greene, "The fabrication and characteristics of three layer $In_{1-x}Ga_xAs_yP_{1-y}$ lasers for CW operation at 1.5 m wavelength," presented at the 6th European Conf. Opt. Commun., York, England, Sept. 1980.

[19] J. Irven, A. P. Harrison, and J. G. Lamb, "Single mode fibre fabrication for a submarine cable system laid in Loch Fyne, Scotland," presented at the 6th European Conf. Opt. Commun., York, England, Sept. 1980.

[20] K. Nakagawa and T. Ito, "A detailed evaluation of an attainable repeater spacing for fibre transmission at 1.3 μm and 1.55 μm wavelengths," *Electron Lett.*, vol. 15, pp. 776–777, Nov. 22, 1979.

John E. Midwinter (M'69) graduated in 1961 from Kings College, London, England, and received the Ph.D. degree from the University of London, London, in 1968.

From 1961 to 1968 he was engaged in research in nonlinear optics and solid-state lasers at the Royal Radar Establishment, Malvern, Worcs. From 1968 to 1970 he was with the Perkin Elmer Corporation, Norwalk, CT, where his research was on nonlinear optics and integrated optics. During 1971 he was with the Allied Chemical Company, Morristown, NJ. In September 1971 he joined the British Post Office Research Centre, now known as the British Telecom Research Laboratories, Ipswich, England, where his research led to the development of the double crucible fiber drawing process and associated measurement and analytical back up. Since 1977 he has been the Head of Optical Communications at the British Telecom Research Laboratories. He is the author of two books, *Applied Nonlinear Optics* and *Optical Fibers for Transmission*, and has published numerous papers.

Dr. Midwinter is a member of the IEE Electronics Division Board and Publishing Committee, and Chairman of the IEE Optics and Infra Red Committee. He has served on the organizing committees of a number of IEEE sponsored meetings–CLEOS, CLEA, ICC, IDEM, and IOOC. He is the Editor of *Optical and Quantum Electronics.*

Authorized licensed use limited to: British Telecommunications via the BT Library. Downloaded on July 21,2025 at 17:03:29 UTC from IEEE Xplore. Restrictions apply.